Experimental Thermal and Fluid Science 35 (2011) 226–233

Contents lists available at ScienceDirect

Experimental Thermal and Fluid Science

journal homepage: www.elsevier.com/locate/etfs

Experimental investigation on resistance characteristics in micro/mini cylinder group

Liu Zhigang *, Zhang Chengwu, Guan Ning

Energy Research Institute of Shandong Academy of Sciences, Jinan 250014, China

ARTICLE INFO

Article history:
Received 25 May 2009
Received in revised form 7 September 2010
Accepted 8 September 2010

Keywords:
Micro/mini cylinder group
Friction factor
Vortex resistance
Scale effect
Roughness effect

ABSTRACT

Friction factors associated with forced flow of de-ionized water over staggered and in-line micro/mini cylinder group plates with 3.5 mm width and 40 mm length, which are made of micro/mini cylinders with hydraulic diameter of 0.5 mm and the heights of 1.0 mm, 0.75 mm, 0.5 mm and 0.25 mm, respectively, have been experimentally investigated over Reynolds number ranging from 25 to 800. The flux and the pressure drop between the inlet and the outlet of micro/mini cylinder group are measured and the experimental results are compared with those of convectional correlations. The investigation shows the value of *fRe* is approximately the constant in micro/mini cylinder group plates when the flow is purely laminar state. Except test sections with 0.25 mm cylinder height, the values of *fRe* for other test sections increase when $Re > 100$, as the results of the appearance of vortex resistance, the enhancement of stream pulse and the acceleration of stream frequency. For test section with 0.25 mm cylinder height, the values of *fRe* rapidly and oscillatingly increase at $Re > 150$ due to the influence of the scale effect, tip clearance effect and the roughness effect on the cylinder surface and bottom of micro/mini cylinder group plates. The friction factor in a staggered array is much larger than that at in-line array for micro/mini cylinder group plates and the higher the cylinder height is, the lower the friction factor becomes.

1. Introduction

The design of micro/mini pin fins (the authors call micro/mini cylinder group when fin's shape is circular) using microfabrication techniques opens new opportunities in Micro-Electro-Mechanical Systems (MEMS), but it requires in-depth understanding of the pertaining heat and fluid flow.

Over the past century, some researchers have explored various heat transfer and pressure drop characteristics for flow across a bank of tubes at macro scale and a considerable amount of data and correlations for heat transfer coefficients (Nusselt number) and friction factors were ready in the literature [1–5]. Explicit correlations for various flow regimes (laminar, transitional, or turbulent), pin fin arrangements (staggered or in-line) and pin geometry including longitudinal/transverse pitch-to-diameter ratio and pin height-to-diameter ratio (L/D) have been developed. Peles et al. [6] investigated heat transfer and pressure drop phenomena over a bank of micro pin fins. The investigation showed the heat transfer and pressure drop correlations were currently not sufficiently developed, but the results strongly suggested that pin fin heat skins deserved adequate research attention. Sparrow et al. [7] have observed that cylinder–endwall interactions penetrated deeper into the free stream flow with a decreasing Reynolds number. Thus, at low Reynolds number the endwall effect was expected to be prevalent over a significantly broader range of H/d values compared with that at high Reynolds numbers. However, the extent of this effect could not be fully determined currently since very few data were available on laminar Reynolds numbers (especially for $Re < 100$). Friction factors, on the other hand, displayed no such deviation for turbulent flow [8], but for laminar flow it was found [9] that the pin fins height-to-diameter ratio played a vital role in determining the friction factor. Kosar et al. [10] experimentally studied pressure drop and friction factors associated with the forced flow of de-ionized water over staggered and in-lined circular/diamond shaped micro pin-fin bundles 100 μm long with hydraulic diameter of 50 μm and 100 μm, the experimental results showed that pin fin height to diameter ratio had a significant effect on the friction factor and staggered tube configuration results in higher friction factors than the in-line configuration. Kosar and Peles [11] experimentally studied the thermal–hydraulic analysis over a bank of micro pin fins, and concomitant results showed acquiring knowledge of the pressure drop/friction faction was vital to understand the mechanism of the convective heat transfer in micro fin pins. In addition, Galvis et al. [12], Qu and Siu [13], Zhang et al. [14], Huang et al. [15] and Sweeney and Meskell [16] numerically investigated the flow and heat transfer characteristics in conventional scale or

* Corresponding author. Tel.: +86 531 85599030; fax: +86 531 82961954.
E-mail address: zgliu9322@yahoo.com.cn (Z. Liu).

0894-1777/$ - see front matter © 2010 Elsevier Inc. All rights reserved.
doi:10.1016/j.expthermflusci.2010.09.005

Nomenclature

a_0, a_1	constant
a_2, a_3	constant
c	constant
C_g	tip clearance, m
d	hydraulic diameter of micro/mini cylinder, m
f	friction factor
G	mass flux, m^2/s
H	cylinder height, m
L	length of cylinder group based plate, m
ΔP	pressure drop between inlet and outlet of micro/mini cylinder group, Pa
Re	Reynolds number
S	distance between cylinders center, m
S_d	inclined distance of based plate, m
S_L	longitudinal distance of based plate, m
S_T	transverse distance of based plate, m
S_w	distance between the test section internal wall and the most lateral cylinders, m
ΔT	temperature difference between inlet and outlet of micro/mini cylinder group, °C
T	fluid temperature, °C
u	fluid velocity, m/s
W	width of cylinder group based plate, m

Greek symbols

ε	ratio of tip clearance to cylinder height
μ	dynamic viscosity, kg/(m s)
ρ	density, kg/m^3

Subscripts

av	average
f	fluid
max	maximum
1	inlet of test section
2	outlet of test section

micro/mini scale fin pins (or cylinder group) for laminar, transitional and turbulent state and they improved the prediction of the flow and heat transfer in fin-pins or cylinder group.

The aforementioned studies provided valuable insight into the pressure drop characteristics of fluid flows across a bank of pin fins at the conventional or micro-scale. It is well known, the flow around circular cylinders is a classical problem of fluid mechanics. When fluid flows around the cylinder, the flow cross-section contracts, the velocity increases and the pressure decrease along the way. At the same time, the cylinder boundary layer separation occurs due to the existence of the viscous forces and thus the flow around cylinder is formed. The vortex shedding among cylinders is the most common flow pattern in the nature, accompanied with the resistance increase, oscillations and negative effects. In addition, the Yong water phenomenon will be generated on the head of cylinder and the pressure at the cylinder is also increased synchronously, which results in the flow around a circular cylinder becoming very complicated. At present, the results of theoretical studies related to the flow around the cylinder are poor, so it is an important and significant work to study the problem of flow around the cylinder theoretically.

The present study is to investigate experimentally the flow characteristics associated with the forced flow of de-ionized water over staggered and in-line micro/mini cylinders group with 500 μm hydraulic diameter and the lengths of 250 μm, 500 μm, 750 μm and 1000 μm, respectively, over Reynolds number ranging from 25 to 850. The influences of various micro/mini-scale effects on the flow characteristic in micro/mini group are systematically analyzed and make explanations for the resistance mechanism in micro/mini cylinder group.

2. Experimental setup and procedure

The schematic of the experimental apparatus is shown in Fig. 1.

As shown, the apparatus is used to supply pressure, which is sourced from a nitrogen bottle of 12 MPa and works at higher pressure than 2 MPa. The pressure supply system is comprised of a pressure supply system, a testing liquid reservoir, a test section and a data acquisition system. The stable and exact pressure nitrogen is supplied by the pressure supply system, which comprises a nitrogen bottle, two pressure meters, a reducing valve, a precise pressure regulating valve and two quick-opening valves. The nitrogen bottle, which is capable of pressure to 12 MPa, can maintain a given pressure precisely (less than 2 MPa) by a pressure-reducing valve. The working fluid of de-ionized water flows through the test section from the liquid pool with the high-pressure nitrogen as a pressure source. The liquid pool is connected by a small-diameter steel tube with 100 MPa resisting pressure to a joint just upstream of the micro/mini cylinder group. Two calibrated pressure transducers and the thermocouples (T-type), which are installed at the two-end joint of the test section, are used to measure the inlet and the outlet pressures and temperatures of the test section and the transducers are zeroed before each test. The fluid flow rate for a given pressure difference and a micro/mini cylinder group sample is determined by collecting the liquid volume during the corresponding elapsed measuring time. An electronic balance is used to measure the weight of the accumulated liquid and the liquid density is calculated based on the average temperature of the inlet and outlet of test section, and thus the liquid volume is obtained. The measurement is initiated after the prescribed experiment pressure is set up by opening the reducing valve in the nitrogen bottle and adjusting the precise regulating valve, then the fluid flow become steady as well as the fluid level in the micro beaker reach a pre-set value. The elapsed time is then recorded while the level in the micro beaker reached a desired increment.

Using precise machining processing, the staggered and the in-line array arrangements micro/mini cylinder group base plates with 40 mm length and 10 mm width are manufactured (material for the copper), as shown in Fig. 2.

A layer thin glass covers the base plate and a 704-silica gel is used to airproof the base plate and the thin glass, so the micro-channels made from micro/mini cylinders are formed. Length L and width W of each base plate are measured by a vernier and their hydraulic diameter of micro/mini cylinder d, cylinder height H, and distance between micro/mini cylinders center S are measured by a micrometer. The hydraulic diameter of the cylinder is about 500 μm in present experiments, and the heights of micro/mini cylinders are listed in Table 1.

The inlet and the outlet temperatures, T_1 and T_2 and pressure drop, ΔP, between the inlet and the outlet are measured during the experimental process. The average temperature of the inlet and the outlet is used as the characteristic temperature and the hydraulic diameter of micro/mini cylinder as characteristic dimension, so the Reynolds number is expressed as:

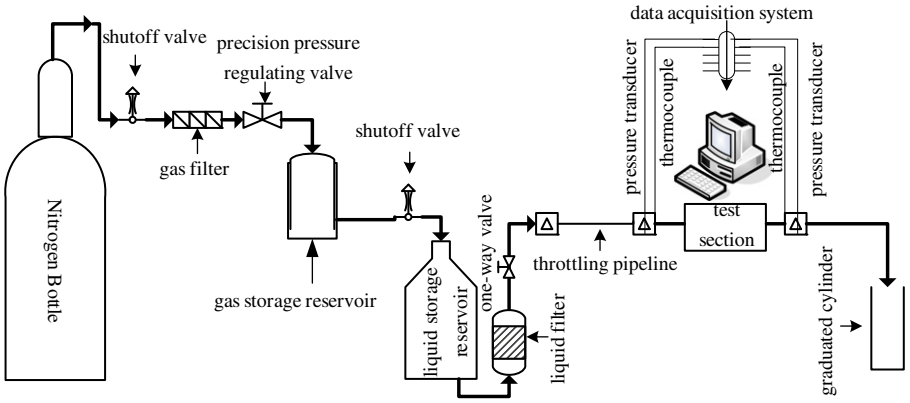

(a) Schematic of micro/mini cylinder group experimental setup

(b) Photo of micro/mini cylinder group experimental setup

Fig. 1. Experimental setup.

$$Re = \frac{\rho u_{\max} \cdot d}{\mu} \tag{1}$$

$$u_{\max} = \frac{GS}{\rho WH(S-d)} \tag{2}$$

In general, the Reynolds number and f are usually calculated based on the minimum cross-sectional flow area, because the pressure drop is dominated by the minimum cross-sectional flow area of micro/mini cylinder group, especially for short cylinders [10].

In present experiments, the main uncertainties come from the measurements of the temperature, the pressure and the geometrical dimension of micro/mini cylinder group. The thermocouples with accuracy of 0.15 °C (less than 100 °C) are used to measure the temperature and the average uncertainties of the entrance and the exit of the micro/mini cylinder group are about ±0.3 °C. The electronic balance with an accuracy of ±0.1 mg is used to measure the flow rate and the uncertainty is less than 0.5% because the tests are conducted with an increment of at least 50 g; the uncertainty of the pressure is less than ±1 kPa for the pressure transducers of CYB-10S type. The geometrical dimension of micro/mini cylinder group is dependent on the accuracy of the engraving machine (YF-DA7060) and its accuracy is ±5 μm, so the relative roughness of the bottom and the cylinder surface is less than 2%.

As mentioned above, the volumetric flow rate is measured using the electronic balance. All other data can be acquired from the data acquisition system. In present experiments, all data must be measured in steady state. When the pressure and the temperature keep a constant level, a stable state has been achieved. The experimental uncertainties of all data are listed in Table 2, and the error analysis method comes from reference literature [17].

3. Experimental results and discussion

In present experiments, the measured parameters are the pressure drop across the micro/mini cylinder group ΔP, the volume flow rate V and the temperature of the working fluid T_f. Other parameters use to describe the friction characteristics in micro/mini cylinder group, and friction factor f can be easily related to these parameters as follows:

$$f = \frac{2\Delta P d}{\rho L u_{\max}^2} \tag{3}$$

The physical properties of water involved in these calculations, such as density ρ, dynamic viscosity μ, are determined by the measured water temperature of the inlet and the outlet in micro/mini cylinder group, respectively. According to the classical theories, the Chilton–Generaux correlation is given to describe flow resistance for the developed laminar flow in cylinder group at staggered state [18],

$$f = \frac{106}{Re} \tag{4}$$

For the in-lined arrays, the flow resistance for laminar flow state can be expressed by Gaddis–Gnielsk correlation [19],

$$f = \frac{280\pi\left\{\left[\left(\frac{S_L}{d}\right)^{0.5} - 0.6\right]^2 + 0.75\right\}}{Re\left(4\frac{S_L S_T}{d^2} - \pi\right)c^{1.6}} \tag{5}$$

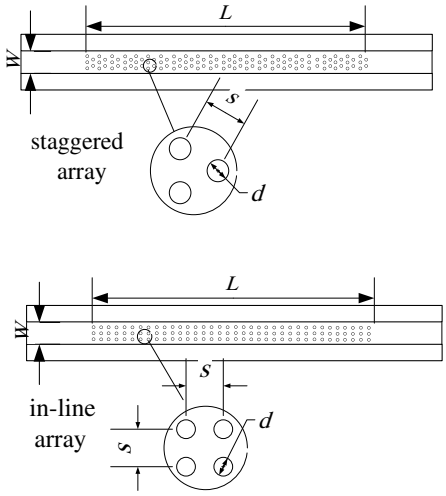

(a) Schematic of micro/mini cylinder group section

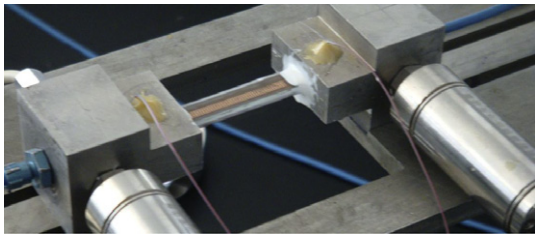

(b) Photo of micro/mini cylinder group section

Fig. 2. Test section of micro/mini cylinder group.

Table 1
Cylinder heights of micro/mini cylinder group (mm).

Serial number	No. 1	No. 2	No. 3	No. 4
Staggered	0.25	0.50	0.75	1.0
Serial number	No. 5	No. 6	No. 7	No. 8
In-line	0.25	0.50	0.75	1.0

Table 2
Experimental uncertainties.

Variable	ΔP	ΔT	G	Re	f
Uncertainty (%)	±0.2	±0.3	±1.1	±2.9	±5.7

where c is defined as:

$$c = \frac{S_T}{d}, \quad \frac{S_L}{d} \geqslant \frac{1}{2}\sqrt{2\frac{S_T}{d}+1}$$

$$c = \frac{S_d}{d}, \quad \frac{S_L}{d} < \frac{1}{2}\sqrt{2\frac{S_T}{d}+1}.$$

It is the 90° angle between flow direction and test section when the working fluid enters into the test section at the middle. The variations of the experimental friction factor with Reynolds number are plotted in Fig. 3 in staggered and in-line arrays. Comparisons are also drawn between the experimental data and the correlations of Chilton–Generaux and Gaddis–Gnielsk.

The variation law of the experimental friction factor is different from that obtained by Eq. (3) with the increase of the Reynolds

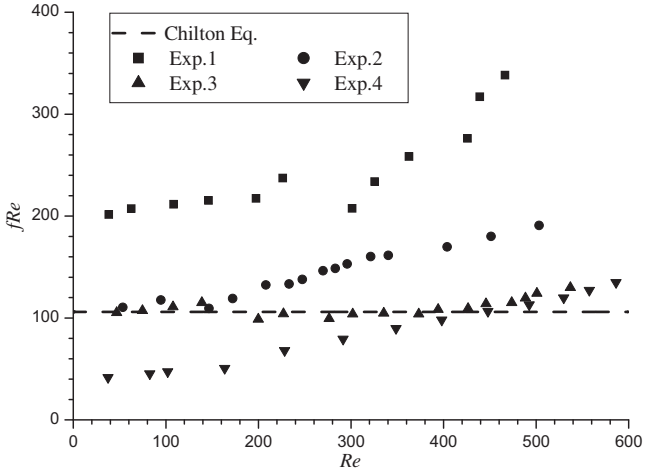

(a) Staggered array

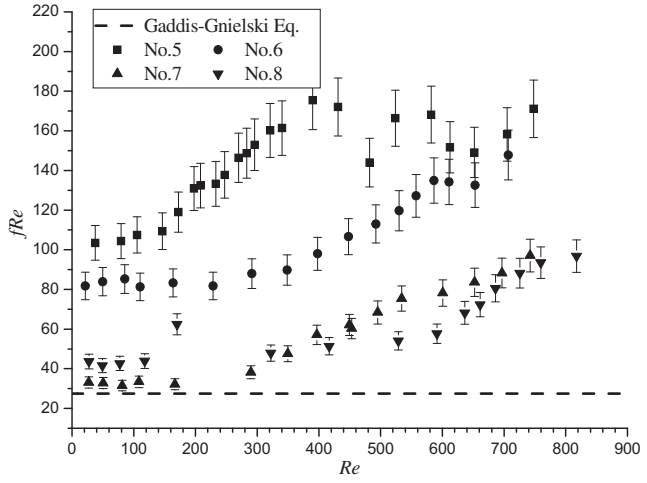

(b) In-line array

Fig. 3. *fRe*–*Re* relationship between experimental results and theoretical values in micro/mini cylinder group.

number, as shown in Fig. 3. From the mechanical viewpoint, the force, which acts on the fluid flow around cylinder, can be divided into two categories: the shear stress of the surface tangent direction and the dynamic pressure of the surface normal direction. Between them, the projection of the role of liquid on the surface frictional resistance at the flow direction is the friction force. The pressure distribution is asymmetry on the cylinder due to the appearance of vortices in cylinder wake zone, so the pressure drop occurs at the flow direction, which is called the vortex resistance [20]. The values of *fRe* not apparently increase with the increase of the Reynolds number at low Reynolds numbers and the flow is a purely laminar flow state in micro/mini cylinder group. At the moment, there is no vortex in micro/mini cylinder group and the resistance comes from the shear stress when water flowed around the cylinder group, not vortex resistance [21]. With the increase of Reynolds number, the values of *fRe* began to smoothly and slightly increase with the increase of the Reynolds number except for the Nos. 1 and 5 test sections at $Re > 150$. According to the literature [22], we can know that Karman Vortex Streets appear in cylinder group, and there is a vortex resistance too.

For the staggered arrays, the interactions among micro/mini cylinders are weak when the flow among micro/mini cylinders is purely laminar state at low Reynolds number, so the inertia force

effect has no influence on the flow, due to which there is no apparently increase of the flow resistance with the increase of the Reynolds number, as indicated in Fig. 3a. With further increase of the Reynolds number, the working fluid flows through the micro/mini cylinder group of staggered array arrangement at comparatively high flow velocity, and it is very easy to produce vortexes or flow turbulence, even the earlier transition from laminar to turbulent flow among micro/mini cylinders due to the frequent change of flow direction and the effect of the inertia force. Moreover, the rear row cylinders are surrounded by the vortexes resulted from the previous row cylinders in micro/mini cylinder group, so the intensity of the water flow pulsation is strengthened and the water fluctuation frequency is also quickened. In addition, the flow direction of the working fluid is contrary to the income flow impacted by the rear row cylinders and consequently, the friction resistance is further increased.

The experimental friction factors of the Nos. 2–4 test sections are within 50% close to those of Chilton–Generaux correlation when the Reynolds number is less than 600. However, the experimental friction factor for the No. 1 test section is far larger than prediction of Chilton–Generaux correlation and the discrepancies between the No.1 and three other test sections can be larger than 100–200% up to about $Re = 500$ between the No.1 and the Nos. 2–4, as a result of some micro-scale effects in the micro/mini cylinder group, such as the surface roughness, the variety of the main impact force and tip clearance.

For the in-lined arrays, the values of fRe are almost constant at $Re < 100$, as shown in Fig. 3b, because the front cylinders and the rear cylinders are on the same line when the flow retains purely laminar state. At the same time, the flow streamline among cylinders keep the straight line, which shows that the influence of the inter-cylinders disturbance on the flow is also small, therefore, the flow resistance is still nearly unchanged even if the effect of the inter-cylinders disturbance.

The values of fRe gradually increase with the increase of the Reynolds number at $Re > 100$ except for the No. 5 test section. At the moment, there may be lots of vortexes among micro/mini cylinder group [21], and the rear row cylinders are not surrounded by the vortexes resulted from the front row cylinder when the diameter of the vortexes is small, so the increase of the flow resistance among cylinder group is not apparent, as shown in Fig. 3b. With the increase of the flow velocity, the diameter of the vortexes will be accordingly increase and the interaction of the front row cylinders on the rear row cylinders becomes apparent when the vortexes' diameter is larger than that of the distance between the cylinders. Moreover, the disturbances, even the turbulence flow may appear in the wake zone of micro/mini cylinders [20]. If the direction of the disturbance in the wake zone is almost the same as that of vortexes, the flow resistance in micro/mini cylinder group will decrease, conversely, there are obviously increase for flow resistance [23]. In addition, there is higher pressure for the front row cylinders compared with the rear row cylinders due to the obstruction effect of the front row cylinders. The pulsation at vortexes zone among the micro/mini cylinders is weak because the flow streamline among cylinders can keep a straight line at low Reynolds number, at the same time, the water level will rise and flow velocity diminishes due to obstruction flow effect of the front cylinders.

As shown in Fig. 3b, the experimental friction factor is close to prediction of the Gaddis–Gnielski correction at low Reynolds number, and with the increase of the Reynolds number, the experimental results become far larger than the theoretical values, especially for the No. 5 test section.

There are considerable difference between the experimental results and the theoretical solutions according to Fig. 3, and the shorter the cylinder heights is, the larger the difference becomes, which shows that the theoretical correlations related to the convectional scale cannot describe the flow characteristics in micro/mini scale cylinders group.

The experimental friction factors for the Nos. 1 and 5 test sections, which are much larger than those of the six other test sections, rapidly increase in oscillation, and the main reasons are as follows:

(1) When the cylinder height reduce to micron-level, the decrement in the flux is the cubical proportional to the decrease in hydraulic diameter and the flow velocity rapidly increase, so the flow will become very unstable for the same Reynolds number.
(2) It is well known, the flow in micro-space is susceptive to the roughness effect [24], and thus the wall surface roughness is the one of the important factors for earlier transition from laminar to turbulent flow. In present experiments, the micro/mini cylinder surface and the bottom surface of the base plate is not absolutely smooth on the micro/mini cylinder surface and on the bottom of the base plate, so it is very easy to present disturbance flow or the earlier transition from laminar to turbulent flow for cylinders group when the flow space is reduced to micro/mini level, as results in the increase of the pressure drop on the cylinders, and then the shear stress resistance is also increased accordingly.
(3) The nonuniformity of the flow allocation will become more apparent among cylinder group with the decrease of the flux per unit volume. Consequently, there are Karman Vortex Streets in cylinders group at lower Reynolds number. The periodic vortex shedding flow will be formed owing to the influence of the cylinders impaction on the Karman vortexes, furthermore, transitional flow even turbulent flow will appear in the wake zone under the impaction of the small disturbance factor of the free stream [25]. On the one hand, the rear micro/mini cylinders are surrounded by the vortexes resulted from the front row micro/mini cylinders, so the intensity of the stream pulsation is strengthened and the frequency of the stream pulsation become faster; on the other hand, the flow direction in the vortexes zone is contrary to that of the free stream [26], so the alternation of the flow directions at the boundary between the vortexes and Karman Vortex Streets. In addition, there are the periodic vortexes shedding flow among cylinders group, which results in the rapid and oscillating increase of the vortexes flow resistance. Therefore, the flow resistance of the Nos. 1 and 5 test sections are remarkably abnormal due to the interaction among the three aspects mentioned above.

The comparison of the friction factors between the staggered array arrangements and the in-lined array arrangements is listed in Fig. 4.

Whether in the staggered array or in the in-line array, the flow in the cylinders group is purely laminar state at lower Reynolds number. However, the friction factor in the staggered array is larger than that in in-line array because the flow distance in the staggered array is longer than that in the in-line array due to the continuous shift of flow direction in the staggered array, as shown in Fig. 4.

As mentioned above, there is longer flow distance in the staggered array due to continuous shifts of flow direction, consequently, it is easier to suffer from the disturbance and give birth to the vortexes, even earlier transition from laminar flow to turbulent flow in the wake zone. Moreover, the rear row cylinders always exist in the vortexes resulted from the front row cylinders at staggered array, so the intensity of the stream pulsation becomes stronger and the frequency is faster at staggered array compared with those at in-line array. The flow direction can be

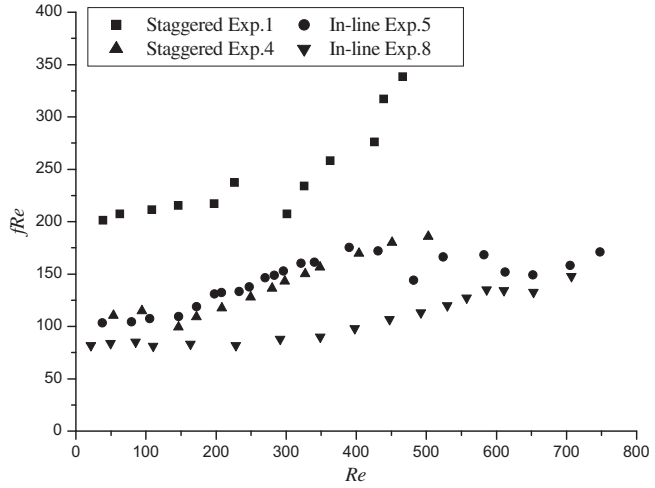

Fig. 4. *fRe*–*Re* relationship between staggered and in-line arrays at laminar state.

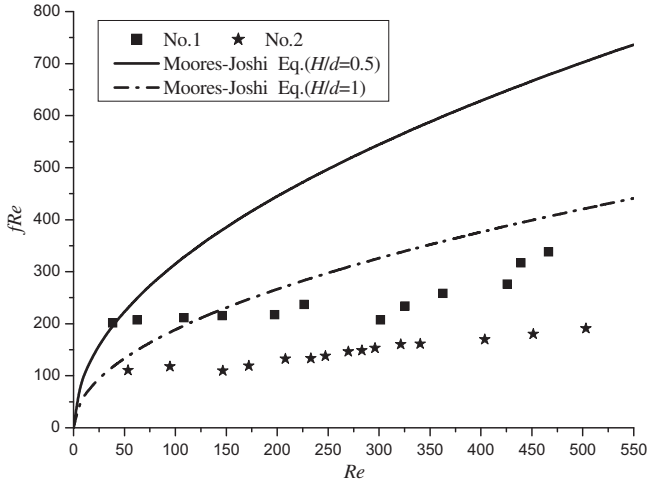

Fig. 5. Influence of height on friction factor in staggered array.

changed due to the obstruction effect of the front row cylinders to the rear row cylinders, as a result of further increase of the flow friction factor at staggered array. Based on above mentioned reasons, the friction factor at staggered array is much larger than that at in-line array in the cylinder group. When hydraulic diameter of the cylinders group is reduced to micron-level, the flow velocity will be very high at the same Reynolds number, so the intensity of the stream pulsation will be stronger and the frequency of the stream pulsation becomes faster. Besides, the flow is susceptible to the influence of the some micro-scale effects, such as the roughness effect, the endwall effect, the dimension effect, and the variety of main acting forcer. It is well known if the relative roughness of channel wall is less than 5%, it has almost nothing on the flow law for conventional channels. However, the very low relative roughness will influence the flow characteristic of micro-space [27], and it will increase the flow resistance in micro-space. According to literature [24,27], the flow resistance can increase up to 10–15% due to the relative roughness less than 2% of micro/mini cylinder surface in micro-space. Literature [10] think the discrepancies between the experimental data and the HEDH correlation [28] for the staggered arrays and the in-line arrays are 17.4% and 21.9%, respectively, due to the endwall effect, and the correlation underpredict the experimental results, which suggests that the endwall effects are significant for $H/D = 1$. In fact, there are still obvious discrepancies between the experimental data and HEDH correlation if endwall effects are neglected, because the correlation cannot accurately predict the experimental results. Of course, the endwall effect will increase flow resistance in micro/mini cylinder group with $H/d = 1$ and the discrepancies resulted from endwall effect may be within 20% according to literature [10] and the theoretical analysis in the paper. Therefore, the friction factors of the No.1 test section are far higher than those of other test sections.

The friction factor becomes higher and higher with the decrease of the cylinder height, and it is different when the height-to-diameter of cylinder begins to become small even if the experimental uncertainties are considered, which illuminated that there is significant influence of the cylinder height on the flow resistance. According to the classical theories, the Moores–Joshi correlation [29] (the correlation is applied to $0.5 \leqslant H/d \leqslant 1$) without tip clearance is given to describe flow resistance for different cylinder heights in the staggered array with the change of the Reynolds number:

$$f = 31.84Re^{-0.502} \quad \text{for } H/d = 0.5$$

$$f = 19.04Re^{-0.502} \quad \text{for } H/d = 1 \qquad (6)$$

The variations of the experimental friction factors of the Nos. 1–2 test sections with the increase of the Reynolds number are plotted in Fig. 5 and the comparisons are also drawn between the experimental data and predictions of Moores–Joshi correlation.

As shown in Fig. 5, the experimental values of the *fRe* remain almost constant with the increase of the Reynolds number at low Reynolds number and the experimental values gradually increase as the Reynolds number increase up to more than 150. Further more, the shorter the cylinder height is, the greater the friction factor becomes. However, the calculating values of the *fRe* increase exponentially with the increase of the Reynolds number, as indicated in Eq. (6). The variation law between the experimental results and calculating values is different, so this discrepancy may be attributed to the tip clearance in test section, especially for abnormal tip clearance.

The schematic of the test sections with and without abnormal tip clearance are shown in Fig. 6.

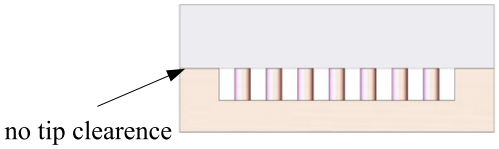

(a) Cross-section of array-no tip clearance

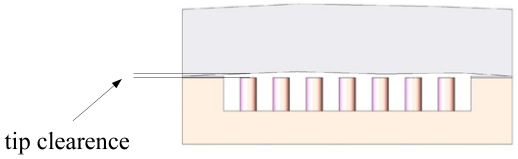

(b) Cross-section of array-with abnormal tip clearance

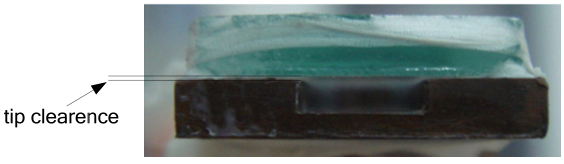

(c) Photo of test section with tip clearance

Fig. 6. Test section with and without tip clearance.

The microchannels made from micro/mini cylinders are formed by a base plate with a thin glass layer cover airproofed by the 704-silica gel, so the tip clearance will be come into being due to an uneven surface of the thin glass and the thickness of the 704-silica gel, as shown in Fig. 6b. The surface irregularity degree of the glass can be measured by a glass flatness measuring instrument (RWG-I /LVDT/DF, Strainoptics Co.) and the thickness of silica gel used a micrometer. In present experiments, the surface maximal irregularity degree of the glass covered in the base plate is about ±29.52 μm and the average thickness of silica gel is 26.8 μm, so the maximal ratio of tip clearance to cylinder height is:

$$\varepsilon_{\max} = \frac{C_g}{H} = \frac{29.52 + 26.8}{500} = 11.26\% \quad \text{for } H = 500\ \mu\text{m}$$

$$\varepsilon_{\max} = \frac{C_g}{H} = \frac{29.52 + 26.8}{250} = 22.52\% \quad \text{for } H = 250\ \mu\text{m}$$

Part of fluids flow through the tip clearance during the experimental process, which can apparently reduce the flow resistance, especially for low cylinder height. The heights of the Nos. 1 and 2 are 250 μm and 500 μm and so the $(C_g/H)_{\max}$ reach 22.52% and 11.26%, respectively. Sparrow et al. [30] employed a duct of constant height with pins of varying length resulting in H/D from 1.75 to 2.5 and C_g/H of 0, 0.11, 0.25 and 0.43. For C_g/H of 0.11, the investigations found f was reduced to 41% of the non-clearance case. However, the experimental data of the Nos. 1 and 2 are about 105% and 90% lower than the calculating values when $Re > 150$, respectively, as shown in Fig. 5. Besides the tip clearance effect, the distance S_w, between the test section internal wall and the most lateral cylinders also apparently affects the flow resistance. The larger the S_w is, the smaller the friction factor becomes according to the experimental results. Obviously, the friction factor will decrease when the S_w is larger than the hydraulic diameter of micro/mini cylinders. In present experiments, the S_w is 2.1 times more than the cylinder diameter, which further decreases the flow resistance of micro/mini cylinder group. Further investigations of the quantitative relationship between the S_w and the flow resistance in micro/mini cylinder group must be conducted in the near future.

In conclusion, the friction factor in micro/mini cylinders group is affected by many factors, so the flow mechanism is exceptional complex. Existing conventional classical correlations cannot describe the flow characteristics in micro/mini cylinder group, therefore, further theoretical analysis and experimental study must be conducted to explore the detailed flow mechanism in micro/mini cylinders group.

4. Conclusion

The friction factor behaviors of de-ionized water flowing through micro/mini cylinder group with hydraulic diameter of 500 μm in the staggered array and at in-line array are investigated experimentally. Experimental tests are carried out in wide range of Reynolds numbers (25–800), and the corresponding friction factors are obtained. Comparisons between the experimental results and predictions of the classical correlations lead to the following concluding remarks:

(1) Whether at staggered array or at in-line array micro/mini cylinder group, the values of the fRe not apparently increase at low Reynolds number;
(2) For the staggered arrays, the intensity of the stream pulsation becomes stronger and the frequency is faster due to the appearance of the vortexes and interactions among the cylinders. The fiction factors in the staggered arrays are far larger than those in the in-line arrays; for the in-line arrays, the vortexes in the micro/mini cylinder group can affect the flow resistance only if the hydraulic diameter of the vortexes is larger than the distance between cylinders;
(3) The tip clearance effect and the S_w can obviously affect the flow resistance of micro/mini cylinder group in present experiments. The larger the values of C_g/H and the S_w are, the smaller the friction factor becomes based on experimental results;
(4) Some micro-scale effects, such as tip clearance effect, roughness effect, and endwall effect, result in obvious discrepancies between experimental results and predictions of theoretical correlations. According to present investigations, the tip clearance effect for test sections with $H/d \leqslant 1$ can reach more than 90% deviation and the roughness effect leads to 15% at most discrepancy. For the endwall effect, it may lead to within 20% deviation from classical correlations.

Acknowledgment

The authors acknowledge the financial support provided by the National Natural Science Foundation (No. 50976062).

References

[1] E.M. Sparrow, J.P. Abrahan, J.C.K. Tong, Archival correlations for average heat transfer coefficients for non-circular and circular cylinders and for spheres in cross-flow, Int. J. Heat Mass Transfer 47 (2004) 5285–5296.
[2] S. Whitaker, Forced convection heat transfer correlations for flow in pipes, past flat plates, single cylinders, single spheres, and for flow in packed-beds and tube bundles, AIChE J. 18 (1972) 361–371.
[3] T. Igarashi, Fluid flow and heat transfer around rectangular cylinders (the case of a width/height ratio of a section of 0.33–1.5), Int. J. Heat Mass Transfer 34 (2) (1991) 893–901.
[4] G.P. Merker, H. Hanke, Heat transfer and pressure drop on the shell-side of tube-banks having oval-shaped tubes, Int. J. Heat Mass Transfer 29 (12) (1986) 1903–1909.
[5] E.M. Sparrow, V.B. Grannis, Pressure drop characteristics of heat exchangers consisting of arrays of diamond-shaped pin fins, Int. J. Heat Transfer 34 (3) (1991) 589–600.
[6] Y. Peles, A. Kosar, C. Mishra, et al., Int. J. Heat Mass Transfer 48 (2005) 3615–3627.
[7] E.M. Sparrow, T.J. Stahl, P. Traub, Heat transfer adjacent to the attached end of a cylinder in crossflow, Int. J. Heat Mass Transfer 27 (1984) 233–242.
[8] J. Armstrong, D. Winstanley, A review of staggered array pin fin heat transfer for turbine cooling applications, ASME J. Turbomach. 110 (1988) 94–103.
[9] B.E. Short, D.C. Price, P.E. Raad, Design of cast pin fin cold walls for air-cooled electronic systems, ASME J. Electron. Packag. 126 (2004) 67–73.
[10] A. Kosar, C. Mishar, Y. Peles, Laminar flow across a bank of low aspect ratio micro pin fins, J. Fluids Eng. 127 (2005) 419–430.
[11] A. Kosar, Y. Peles, Thermal–hydraulic performance of MEMS-based pin fin heat sink 128 (2006) 121–131.
[12] E. Galvis, A. Jubran, F. Xi, et al., Numerical modeling of pin-fin micro heat exchangers, Heat Mass Transfer 44 (2008) 659–666.
[13] W.L. Qu, H.A. Siu, Experimental study of saturated flow boiling heat transfer in an array of staggered micro-pin-fins, Int. J. Heat Mass Transfer 52 (2009) 1853–1863.
[14] P.F. Zhang, J.J. Wang, L.X. Huang, Numerical simulation of flow around cylinder with an upstream rod in tandem at low Reynolds numbers, Appl. Ocean Res. 28 (3) (2006) 183–192.
[15] Z. Huang, J.A. Olson, R.J. Kerekes, S.I. Green, Numerical simulation of the flow around rows of cylinders, Comput. Fluids 35 (2006) 485–491.
[16] C. Sweeney, C. Meskell, Fast numerical simulation of vortex shedding in tube arrays using a discrete vortex method, J. Fluid Struct. 18 (2003) 501–512.
[17] R.J. Moffat, Describing the uncertainties in experimental results, Exp. Thermal Fluid Sci. 1 (1988) 3–17.
[18] T.H. Chilton, R.P. Generaux, Pressure drop across tube banks, Trans. Am. Inst. Chem. Eng. 29 (1933) 161–173.
[19] E.S. Gaddis, V. Gnielski, Pressure drop in horizontal cross flow across tube bundles, Int. Chem. Eng. 25 (1) (1985) 1–15.
[20] H.R. Zhu, D.C. Xu, Heat transfer and pressure drop of short pin-fin array with different diameter and shape, J. Aero. Pow. 17 (2) (2002) 246–249.
[21] Y.L. Wang, Y.Z. Liu, G.P. Miao, Three-dimensional numerical simulation of viscous flow around circular cylinder, J. Shang hai Jiao Tong Univ. 35 (1) (2001) 1464–1469.
[22] H.M. Badr, Laminar combined convection from a horizontal cylinder-parallel and contra flow regimes, Int. J. Heat Mass Transfer 27 (1) (1984) 15–27.

[23] Z.Y. Guo, S. Wang, Novel concept and approaches of heat transfer enhancement, in: Proceedings of symposium on energy engineering in the 21st century, Begell House, New York, 2002, pp. 118–126.
[24] Z.G. Liu, X.B. Zhao, C.W. Zhang, Y.L. Hou, Flow and heat transfer in rough micro steel tube, Exp. Heat Transfer 20 (4) (2007) 289–306.
[25] H.D. Nguyen, S. Paik, R.W. Douglass, Unsteady mixed convection about a rotating circular cylinder with small fluctuations in the free-stream velocity, Int. J. Heat Mass Transfer 39 (3) (1996) 511–525.
[26] K.S. Chang, H.Y. Sa, The effect of buoyancy on vortex shedding in the near wake of a circular cylinder, J. Fluid Mech. 220 (1990) 253–266.
[27] Z.X. Li, D.X. Du, Z.Y. Guo, Experimental study on flow characteristics of liquid in circular microtubes, Microscale Therm. Eng. 7 (2003) 253–265.
[28] J. Taborek, Shell and tube heat exchangers: single phase Flow, Handbook of Heat Exchanger Design, Hemisphere, New York, 1983 (Chapter 3.3).
[29] K.A. Moores, Y.K. Joshi, Effect of tip clearance on the thermal and hydrodynamic performance of a shrouded pin-fin array, J. Heat Transfer 125 (2003) 999–1006.
[30] E.M. Sparrow, J.W. Ramsey, Heat transfer and drop pressure for a staggered cylinder wall attached array of cylinders with tip clearance, Int. J. Heat Mass Transfer 21 (1978) 1369–1377.